

UCSF

UC San Francisco Electronic Theses and Dissertations

Title

Epithelial TNF controls cell differentiation and CFTR activity to maintain intestinal mucin homeostasis

Permalink

<https://escholarship.org/uc/item/3r50q5xf>

Author

Reyes, Efren A

Publication Date

2022

Peer reviewed|Thesis/dissertation

Epithelial TNF controls cell differentiation and CFTR activity to maintain intestinal mucin homeostasis

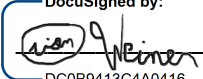
by
Efren Reyes

DISSERTATION
Submitted in partial satisfaction of the requirements for degree of
DOCTOR OF PHILOSOPHY

in
Biochemistry and Molecular Biology

in the
GRADUATE DIVISION
of the
UNIVERSITY OF CALIFORNIA, SAN FRANCISCO

Approved:

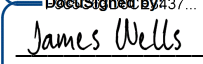
DocuSigned by:

DC0B9413C4A0416... Orion Weiner
Chair

DocuSigned by:

Zev Gartner

DocuSigned by:

Ophir Klein

DocuSigned by:

5F2F4D1A06164C2... James Wells

Committee Members

ACKNOWLEDGEMENTS

I would first like to establish that the completion of my PhD would not have been possible without the love, support, and sacrifice of my family, friends, and colleagues. The impact the following people have had on my personal and professional life is immense and they have all made me a better person and scientist in their own special way.

To my parents, the hardest working people I know, I am so grateful for you both. You instilled a strong work ethic in me since I was a child and encouraged me to choose my own path. In all my years of life, there was never a single time when I felt I did not have your love or support. Mom and Dad, you were and will continue to be my biggest role models. I hope I can one day become the selfless, loving, supportive parents you so genuinely are.

To my grandparents Moncerate Reyes and Victoriano Reyes, I am so grateful to have been able to spend so much time getting to know you as I was growing up. Thank you for helping our family by watching me and taking me to school all those mornings, while my parents were at work. During that time of my life, it meant so much seeing my report cards take a permanent residency on your refrigerator. Thank you for celebrating my accomplishments with such pride and for absolutely spoiling me.

To my older sisters Dee and Jen, I have had some of the best times of my life with you growing up and have created countless fond memories that I will always look back on. I will never forget you taking me to Mission College to register for classes or using your hard-earned money to buy your little bro new shoes and treat him to a movie. Above all, I will remember the times at home, when our maturity level would lower just a bit and

our inner kids would come out. You always thought of me, protected me, and kept me grounded.

To Debbie, my partner in life, you have this radiating energy that always puts a smile on my face, even when times are bad. You encourage me every day and remind me to celebrate my wins no matter how small. You are always helping me in any way you can and have motivated me to be a more compassionate and trusting person. I am so grateful to have you in my life.

Tetrad class of 2014, I consider myself lucky to have gone through grad school with all of you. The hangouts, trips, happy hours, and strong sense of comradery pushed me forward to the end. 1260 house, thank you for the laughs, the dining room table chats, Halloweens, and for easing the pain of the pandemic quarantine. To my college friends, I have known you for 14 years and have grown so much together with you. I am grateful for all the real talk and trash talk and meals you covered because I was a broke graduate student. Looking forward to many more years of friendship, laughs, and life milestones.

Thank you, Dr. Kelly Doran, for allowing an undergraduate with no technical skills like me into your lab. You believed in me even when I didn't believe myself. Thank you to my graduate student mentor Brandon Kim, who was extremely patient with my training and gave me a strong lab foundation to build from. I appreciate Dr. David Traver and Natasha Del Cid for graciously teaching me zebrafish genetics with no prior experience and for supporting me during the tumultuous times of grad school applications.

To Zev Gartner and Ophir Klein, trainees are lucky to have one good mentor, but I somehow managed to find two excellent mentors in both of you. Zev, your excitement for science is infectious and your outside-the-box thinking, is something I deeply admire and

aspire to further develop. Thank you for pushing me to dream big and for giving me the freedom to explore. Ophir, you are one of the kindest people I have ever met and I thank you for always advocating for me. Amongst other things, you have taught me how to take a step back and see the bigger picture, to have confidence in myself, and to network and collaborate.

David Castillo-Azofeifa, I cannot thank you enough. Simply put I would not be the scientist I am today without your mentorship. Amongst the countless technical skills, you patiently taught me, you also gave me my voice. When I first started my PhD I had imposter syndrome and lacked the scientific confidence to even ask questions during lab meetings. You provided a space for me to be heard and consistently encouraged me to participate and share my thoughts. I owe my newfound confidence and sense of belonging in science to you.

To my committee, thank you for pushing me to do the best science I could and for all your useful input and support. To the Klein lab and Gartner lab, thank you for your feedback, eagerness to help, and kind-heartedness. Doing my PhD in such supportive environments made it feel like I was never alone and made it possible to continue onward and finally finish. I would especially like to acknowledge Pauline Marangoni from the Klein lab for always being so mindful and considerate of myself and others. Thank you for advocating for me and for taking on the massive list of responsibilities that you have. Finally, thank you to all the custodial staff, LARC staff, and other UCSF staff whom I had the pleasure of crossing paths with. In the UCSF community, the collaborative nature, openness, and warm environment drew me to UCSF for my graduate studies and will surely make it very difficult to leave. Thank you all!

CONTRIBUTIONS

The content in this dissertation is reformatted from a manuscript currently under journal review at the time of this dissertation submission:

Reyes, E.* , Castillo-Azofeifa, D. * , Gartner, Z.J., and Klein, O.D. Epithelial TNF controls cell differentiation and CFTR activity to maintain intestinal mucin homeostasis. 2022.

Manuscript under review.

*Co-first authors

**Epithelial TNF controls cell differentiation and CFTR activity to maintain
intestinal mucin homeostasis**

Efren Reyes

ABSTRACT

The gastrointestinal tract relies on the production, maturation, and transit of mucin to protect against pathogens and to lubricate the epithelial lining. However, the molecular and cellular mechanisms that regulate mucin production and movement are unclear. Here, we report that the inflammatory cytokine tumor necrosis factor (TNF), which is generated by the epithelium, contributes to mucin homeostasis by regulating both cell differentiation and cystic fibrosis transmembrane conductance regulator (CFTR) activity. Using genetic mouse models, we found that loss of epithelial TNF promoted differentiation of secretory progenitor cells into mucus-producing goblet cells. Furthermore, co-treatment of intestinal organoids with recombinant TNF and a CFTR inhibitor demonstrated that TNF promotes ion transport and luminal flow via CFTR. The absence of TNF led to slower gut transit times, which we propose results from increased mucus accumulation coupled with decreased luminal fluid pumping. These findings point to a TNF-CFTR signaling axis in the adult intestine and identify epithelial-derived TNF as an upstream regulator of mucin homeostasis.

TABLE OF CONTENTS

Chapter 1: Introduction.....	1
Chapter 2: TNF ligand and its receptors TNFR1 and TNFR2 are spatially zonated along the crypt-villus axis	6
METHODS.....	7
Chapter 3: Absence of TNF causes defects in luminal mucin, goblet cell number, gut transit time, and bacterial load	11
METHODS.....	12
Chapter 4: TNF does not affect secretory cell turn-over, but controls goblet cell number by regulating secretory progenitor cell differentiation	16
METHODS.....	18
Chapter 5: Epithelial-derived TNF is required for mucin and goblet cell homeostasis	21
METHODS.....	22
Chapter 6: Epithelial-derived TNF modulates CFTR induced fluid pumping and Meprin- β shedding, which are required for proper mucin flux	26
METHODS.....	28
Chapter 7: Discussion	33
References	37

LIST OF FIGURES

Figure 2.1. RNAscope reveals distinct patterns of mRNA transcript localization for TNF, TNFRI, and TNFR2 in the mouse small intestine.....	10
Figure 2.2. Immunohistochemistry of TNF, TNFR1, and TNFR2.....	10
Figure 3.1. Global loss of <i>Tnf</i> leads to an increase in luminal mucin, but not cellular mucin.....	14
Figure 3.2. Absence of <i>Tnf</i> causes an increase in crypt goblet cell number.....	14
Figure 3.3. Loss of <i>Tnf</i> causes increased gut transit time.....	15
Figure 3.4. Absence of <i>Tnf</i> leads to increased bacterial load in the intestine.....	15
Figure 4.1. Experimental design.....	19
Figure 4.2. Secretory progenitor cell displacement after 48 h is unaffected in <i>Tnf</i> ^{-/-} mice.....	19
Figure 4.3. Loss of <i>Tnf</i> results in an increase in secretory progenitors.....	20
Figure 4.4. Secretory progenitors increase at the expense of absorptive progenitors upon loss of <i>Tnf</i>	20
Figure 5.1. Experimental design.....	23
Figure 5.2. Intestinal epithelial-specific ablation of <i>Tnf</i> reproduces luminal mucin defects seen in global ablation studies.....	23
Figure 5.4. Loss of epithelial TNF results in slower gut transit.....	24
Figure S5.1. <i>Villin</i> ^{CreERT2} ; <i>Tnf</i> ^{flox/flox} mice show no defects in intestine length.....	25
Figure S5.2. <i>Villin</i> ^{CreERT2} ; <i>Tnf</i> ^{flox/flox} mice maintain total goblet cell number.....	25
Figure 6.1. <i>Cftr</i> is expressed in mouse epithelial crypts and intestinal organoids.....	31
Figure 6.2. TNF promotes intestinal organoid fluid pumping via CFTR.....	31

LIST OF FIGURES CONTINUED

Figure 6.3. rTNF treatment of organoids modulates forskolin induced swelling in a
PKC dependent manner..... 32

Figure 6.4. Epithelial TNF regulates Meprin- β shedding..... 32

LIST OF ABBREVIATIONS

CFTR	Cystic Fibrosis Transmembrane Conductance Regulator
EdU	5-Ethynyl-2'-deoxyuridine
FSK	Forskolin
LGR5	Leucine Rich Repeat-Containing G Protein-Coupled Receptor 5
NICD	Notch Intracellular Domain
rTNF	Recombinant TNF
UEA1	Ulex Europaeus (Gorse) Agglutinin I

Chapter 1: Introduction

The small intestinal epithelium serves as both the absorptive surface of the tissue and as a barrier to pathogens and toxins (1). The gut lining is folded into invaginations that house multipotent stem cells, known as crypts, and long finger-like protrusions termed villi, which facilitate nutrient absorption. The intestine is exposed to the external environment through ingestion, and its epithelial barrier prevents entry of toxins and pathogens and restricts resident commensal microbes to the intestinal lumen (2).

The intestinal epithelium comprises a variety of specialized cell types that derive from Leucine-Rich Repeat Containing G Protein-Coupled Receptor 5 (Lgr5)⁺ stem cells (3). Stem cells give rise to highly proliferative absorptive and secretory progenitor cells, which in turn give rise to differentiated cells that perform specialized functions. Absorptive progenitors differentiate into enterocytes that absorb nutrients (1), whereas secretory progenitors give rise to Paneth, goblet, tuft, and enteroendocrine cells that release protective and regulatory factors (1). Paneth cells at the crypt bottom produce antimicrobial peptides (AMPs) that protect the epithelium from bacteria; enteroendocrine cells in the villus produce hormones that regulate digestion and absorption; tuft cells coordinate host immune responses; and goblet cells in the crypt and villus produce the majority of mucin in the intestine (4).

Mucins polymerize to make up the tissue mucus layer, which creates a physical protective barrier that traps pathogens and contaminants to protect the epithelium (5). In addition, the mucus layer serves as a lubricant for the passage of digested food and waste through the gut (6). The small intestine has a single loose mucus layer that is easily removed and is penetrable to bacteria, whereas the mucus of the large intestine has two

layers: a loose outer layer penetrable by bacteria and a dense attached inner layer that is impenetrable to bacteria (6). Despite a loose penetrable mucus layer, the small intestine still manages to separate pathogens from the epithelium via diffusion of antimicrobial peptides released from Paneth cells at the crypt base (7). The mucus itself is thought to act as a diffusion barrier that keeps AMPs close to the epithelium and concentrates AMP most highly at the crypt base. The diffusion barrier further limits the movement of bacteria to the epithelium as well. Mucus is roughly 95% water, therefore the organization and structure of mucin protein building blocks are crucial to maintaining the high water content of mucus (5, 7).

Mucins are a family of proteins that are highly glycosylated, which enables efficient binding of water molecules. At least, 50% of mucin's protein mass is made up of O-glycans which bind to mucin domains, rich in the amino acids Proline, Threonine, and Serine (PTS) (7). Structurally, mucins can be thought of as long, stiff, voluminous rods with a central protein core analogous to the structure of bottle brushes (5, 6). The extensive branching of glycans and binding of water gives mucins their gel-like properties (6). The tips of these glycan networks serve as binding sites for microbes. Interestingly, glycans are extremely diverse in humans along the proximal and middle intestine, which can in part explain the microbial diversity seen among humans (7). However, the microbial communities in the distal intestine are much more uniform. Glycans permit an expanded diversity of mucin binding sites, despite the same core composition of mucin building blocks.

In general, mucins can be classified into two major groups: secreted polymer forming mucins or transmembrane mucins. Polymer-forming mucins undergo homo

oligomerization and form a flexible network and transmembrane mucins remain attached to the apical membrane of the epithelium and form a carbohydrate-rich layer called the glycocalyx, which serves as an additional protective barrier (2). Transmembrane mucins also contain an intracellular domain that can contribute to cell signaling. In the intestine, MUC2 is the major polymer forming mucin and MUC13 and MUC17 are the major transmembrane mucins (6). The turnover of these mucin proteins is crucial to homeostasis, which is exemplified in the fast renewal of the secreted mucin MUC2 (4 h) and the transmembrane mucin MUC17 (24 h) in the small intestine (8).

Defects in mucin homeostasis, seen in diseases such as cystic fibrosis, result in accumulation of mucin, increased bacterial load, and a significant decrease in the rate of food and waste transit (9, 10). Once mucin is produced, the activity of the chloride anion channel CFTR (11) and the protease Meprin- β (12) promote mucin unfolding and shedding, respectively. Whether and how upstream molecular and cellular mechanisms regulate the production and mobilization of mucin during homeostasis remains unclear. An appealing hypothesis is that cytokines can control this homeostatic process, given that they have been extensively shown to modulate goblet cell number and function under pathogenic conditions (6).

For example, during parasitic helminth infection, levels of the cytokine interleukin-13 significantly increase resulting in elevated STAT6 signaling and goblet cell hyperplasia (6). In addition, knockout of interleukin-22 abrogates the goblet cell hyperplasia and mucin filling that typically follows infection with the pathogens *Nippostrongylus brasiliensis* and *Trichuris muris*. Finally, overexpression of interleukin-9 is sufficient to induce goblet cell hyperplasia (6). Various studies also point to the cytokine TNF as a potential regulator of

goblet cell and mucus biology. However, much remains to be learned, as TNF has been predominantly studied in the context of cell death and inflammation in the intestine (13, 14), and its function in non-disease states and homeostasis is less clear (15), with conflicting reports about the relationship between TNF and mucin.

Some studies report that TNF promotes transcription of *Muc2* (16), the major component of mucin, while others assert that it decreases the production and thickness of the mucus layer (17, 18). Developmental studies have also shown divergent results (19, 20), and interpretation of data from *in vitro* studies has been limited by the use of colon cancer cell lines, which lack intestinal cell type diversity and crypt-villus architecture (21). Thus, the role of TNF in adult intestinal homeostasis and mucin production, and the cell types that produce and respond to TNF signals, are unknown.

TNF is a prototypic ligand that is expressed as a transmembrane protein that is cleaved by ADAM17 protease to produce its soluble form. Soluble TNF trimerizes and can interact with both of its cognate receptors, TNFR1 and TNFR2. Generally, TNFR1 is thought to promote pro-death signals and TNFR2 is thought to promote pro-survival signals (22). In the intestine, TNFR1 has been extensively shown to promote villus cell death (23) and TNFR2 has been shown to promote MUC2 transcript expression (16), although the role of TNFR2 is much less clear.

In this study, we aimed to elucidate the cellular source and functional role of TNF during mucin homeostasis by examining adult intestinal tissues and using intestinal organoids that more closely recapitulate *in vivo* physiology than do 2D cell line models (24). RNA *in situ* hybridization and immunohistochemical analysis revealed that Paneth cells are the major epithelial producers of TNF. Genetic studies demonstrated that loss

of TNF led to mucin accumulation and slower gut transit time. By combining genetic ablation of TNF with lineage tracing of progenitor cells, we found that TNF is required for maintaining the proportion of secretory and absorptive progenitors and for suppressing a goblet cell differentiation bias. Using live imaging, we determined that TNF regulates luminal fluid pumping in organoids by modulation of CFTR activity, establishing a TNF-CFTR signaling axis for mucin flux in the intestine. Together, our data indicate that TNF contributes to mucin homeostasis by regulating both secretory cell differentiation into goblet cells and mucin maturation through the activity of CFTR and Meprin- β .

Chapter 2: TNF ligand and its receptors TNFR1 and TNFR2 are spatially zoned along the crypt-villus axis

To identify sender-receiver signaling relationships between cells in the small intestine, we assessed the mRNA and protein expression of the ligand TNF and its receptors TNFR1 and TNFR2. We utilized probes for single-molecule RNA *in situ* hybridization (RNAscope) targeting *Tnf* (encodes TNF), *Tnfrsf1a* (encodes TNFR1), and *Tnfrsf1b* (encodes TNFR2) to visualize mRNA expression in the adult intestine (Figure 2.1, A-C). We also examined protein abundance using immunohistochemistry (Figure 2.2, A-C). TNF, TNFR1, and TNFR2 proteins were widely expressed in the mesenchyme, where major producers of TNF such as macrophages reside (25). In the epithelium, TNF protein expression was more spatially restricted. LysZ⁺ Paneth cells highly expressed TNF, which localized to intracellular granules (Figure 2.2, A), indicating that Paneth cells are a major epithelial producer of TNF and consistent with previous *in situ* hybridization studies (26, 27).

The expression of TNF receptors was also spatially restricted. Ulex europaeus agglutinin 1 (UEA1) is a lectin that labels goblet cells with high intensity and mature Paneth cells with lower intensity (28). By combining UEA1 and TNFR1 stains, we found that TNFR1 was enriched in UEA1⁺ Paneth cells and UEA1⁺ goblet cells (Figure 2.2, B), while TNFR2 was highly expressed in the crypt domain compared to villus cells (Figure 2.2, C). Our data suggest that Paneth cells can both produce and respond to TNF ligand, whereas goblet cells and non-Paneth crypt cells can only respond to the ligand. These findings demonstrate a highly zoned expression pattern of TNF ligand and its receptors,

which may permit different cellular responses to the same TNF signal across the crypt-villus axis.

METHODS

Tissue preparation for immunofluorescence and immunohistochemistry

Animals were anesthetized via intraperitoneal (i.p) injection of 250 mg/kg of body weight avertin (2,2,2-tribromoethanol) and transcardially perfused with 4% paraformaldehyde (PFA) diluted in 1x phosphate buffered saline (PBS). Tissues were post-fixed for 24 h at 4 °C, and processed for paraffin embedding following standard procedures.

Tissue preparation for RNAscope

The ileum was isolated and immersion fixed in 4% PFA for 24 hours at room temperature. The tissue was then processed for paraffin embedding following standard procedures.

Immunofluorescence and immunohistochemistry

Slides containing 7 µm sections from paraffin embedded tissue were heated at 60 °C for 30 minutes until wax was melted. After rehydration, antigen retrieval was performed using Sodium Citrate buffer pH 6.0 or Tris-EDTA pH 9.0 in a pressure cooker for 15 minutes. Sections were then blocked for 2 hours at room temperature in 5% normal goat serum (005-000-121, Jackson ImmunoResearch). Next, slides were incubated in primary

antibody overnight at 4 °C at the listed concentrations. The next day tissues were stained in secondary antibody for 2 hours at room temperature at the listed concentrations. Finally, slides were stained with DAPI (5 µg/ml; D9542, Sigma) for 20 minutes at room temperature and mounted in Prolong Gold Antifade Medium (P36930, Thermo Fisher Scientific). Primary antibodies were used at the following dilutions: rat anti-E-Cadherin (1/200; 13-1900, Thermo Fisher), rabbit anti-E-cadherin (1/350; 3195s, Cell Signaling), rabbit anti-Lysozyme (1/500; A0099, Dako), rabbit anti-Muc2 (1/250; NBP1-31231, Novus Biologicals), rabbit anti-TNF α (1/250; ab6671, Abcam), rat anti-TNF α (1/250, 506302, Biolegend) rabbit anti-TNFR1 (1/250; ab19139, Abcam), rabbit anti-TNFR2 (1/250; PA5-80159, Thermo Fisher), rabbit anti-RFP (1/250; 600-401-379, Rockland), and chicken anti-RFP (1/250; 600-901-379 Rockland).

Secondary stains and antibodies were used at the following dilutions: UEA1-FITC (50 µg/ml; L9006-1 mg, Sigma), UEA-1 rhodamine (1/250; RL-1062-2, Vector Biolabs), Alexa Fluor conjugated secondary antibodies (1/250; A-11034, A-21429, A-21245, A-21247, A-21432, Thermo Fisher), and goat biotinylated secondaries (1/250-1/1000; BA-1000-1.5, BA-9200-1.5, Vector Biolabs)

For immunostaining requiring signal amplification, TSA Cy3 Amplification kits were used (SAT704A001EA, Perkin Elmer) and manufacturer-provided protocols were followed.

Imaging of tissue sections

Image acquisition of immunostained intestinal swiss rolls used for quantitative analysis was performed on a Leica DMI8 inverted microscope at 20x magnification. Image

acquisition of representative regions of immunostained slides was performed using a Zeiss LSM 900 using a 40x objective. A 7 μm z-stack was taken per region (z-step= 1 μm).

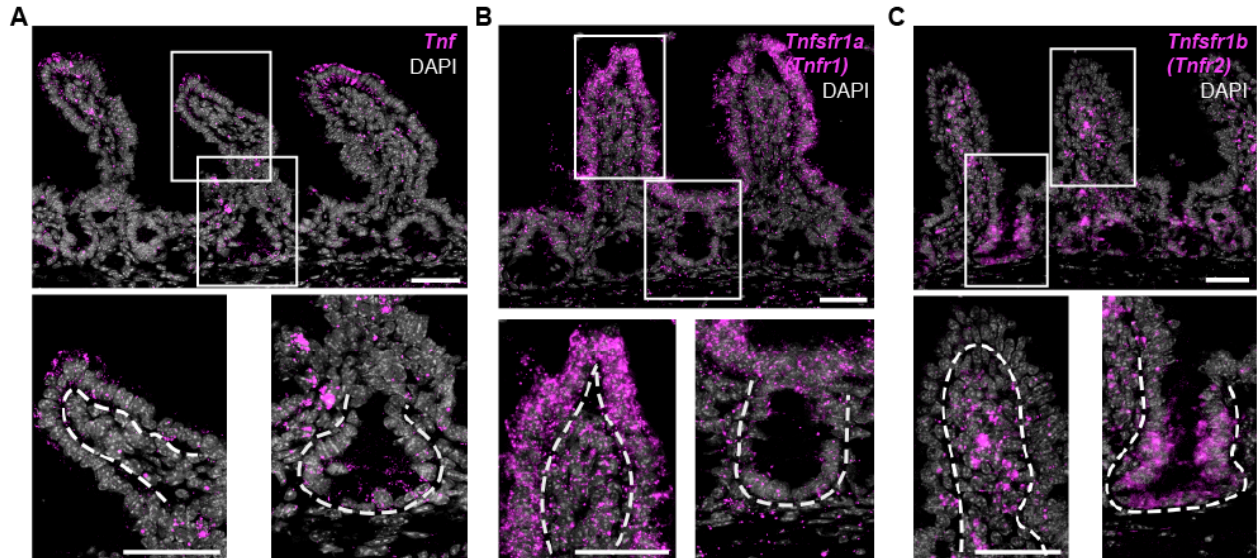


Figure 2.1. RNAscope reveals distinct patterns of mRNA transcript localization for TNF, TNFR1, and TNFR2 in the mouse small intestine. (A) *Tnf* transcripts localize to the villus tip and the crypt base. (B) *Tnfsfr1a* transcripts are broadly expressed in the epithelium. (C) *Tnfsfr1b* transcripts are enriched in epithelial crypts compared to villi. White boxes highlight insets. Dashed lines outline the epithelial-mesenchyme border. Scale bars = 50 μ m.

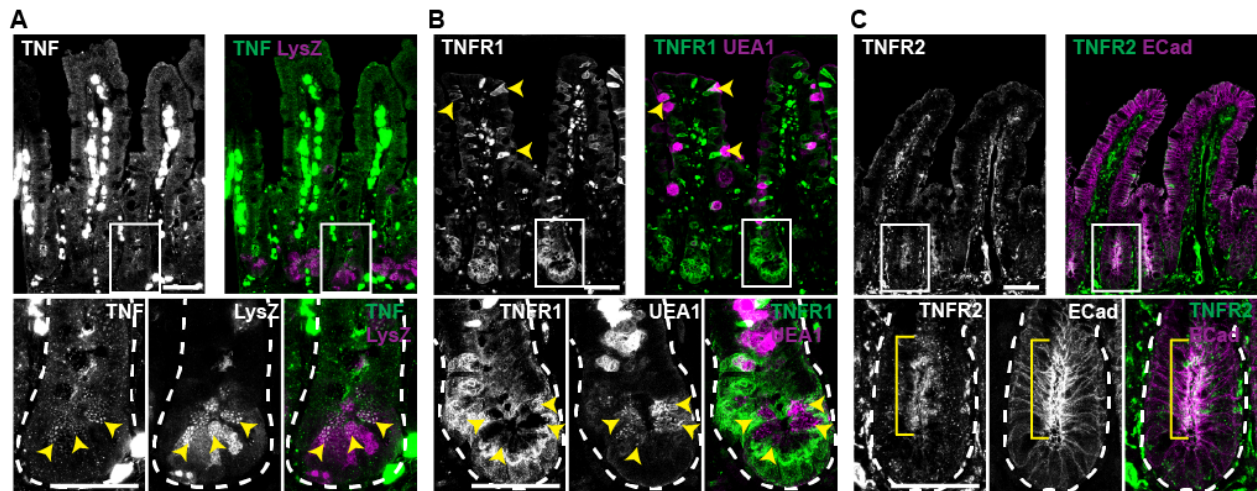


Figure 2.2. Immunohistochemistry of TNF, TNFR1, and TNFR2. (A) TNF expression is highest in *LysZ*⁺ Paneth cell granules (yellow arrows). (B) TNFR1 expression is enriched in *UEA1*^{Lo} Paneth cells in the epithelial crypt and *UEA1*^{Hi} goblet cells in the epithelial crypt and villus (yellow arrows). Contrast is increased in zoom insets to show *UEA1* expression in Paneth cells. (C) TNFR2 is enriched in crypt cells (yellow brackets). White boxes represent zoom insets. Dashed lines outline the epithelial-mesenchyme border. Scale bars = 50 μ m. N = 3 mice per probe.

Chapter 3: Absence of TNF causes defects in luminal mucin, goblet cell number, gut transit time, and bacterial load

Elevated levels of TNF in Crohn's disease tissue samples or treatment of colon cell lines with exogenous TNF cause decreased abundance and thickness of the mucus barrier (18, 29, 30), suggestive of a role for TNF in maintaining intestinal mucus. However, whether and how TNF might regulate mucin production under homeostatic conditions is unclear. We therefore evaluated the role of TNF in mucin homeostasis by analyzing constitutive *Tnf*^{-/-} mice (31), which lack TNF in all tissues, including the intestinal mesenchyme and epithelium. In comparison with age-matched control mice, luminal mucin was elevated in *Tnf*^{-/-} mice (Figure 3.1, A and B). However, intracellular epithelial mucin measured by mean mucin fluorescence (Figure 3.1, C) and granule size per goblet cell (Figure 3.1, D) were unaffected. These findings suggested that increased luminal mucin levels in mutant mice could be explained, at least in part, by an increase in mucus-producing goblet cells. We quantified goblet cell number in control and mutant villi and found that, while the total number of goblet cells remained constant (Figure 3.2, B), mutant mice had more goblet cells in crypts (Figure 3.2, C).

Prior work has correlated increased luminal mucin with increased gut transit time (10). Therefore, we tested if gut transit time was delayed in *Tnf*^{-/-} mice. Using a 70 kD FITC-Dextran dye, we tracked anteroposterior dye displacement along the gut length over time (Figure 3.3, A). After 1 hour, FITC-Dextran traveled 80 percent of the total gut length of control mice and 70 percent of the total gut of mutant mice (Figure 3.3, B); total gut length remained constant between both groups (Figure 3.3, C). These findings indicate that, in the absence of TNF, the expulsion of digested food and waste is impaired.

Together with slower gut transit, increased luminal mucin is correlated with higher levels of bacterial load (32). Therefore, we assessed the bacterial load of control and mutant mice by isolating genomic DNA from feces and performing qPCR for the universal bacterial 16s rRNA gene, which showed that bacterial load in mutant mice was elevated ~ 20-fold (Figure 3.4, A). Thus, during homeostasis, TNF contributes to the regulation of intestinal mucin levels, goblet cell number, gut transit, and bacterial load.

METHODS

Mice

Tnf^{-/-} (Jax: 005540; Pasparakis et al., 1996), *Rosa26*^{tdTomato} (Jax: 007905, Madisen et al., 2010), and *Vil*^{CreERT2} (Jax: 020282; el Marjou et al., 2004) mice were purchased from the Jackson Laboratory and maintained on a C57BL/6 background. Additional mouse lines include combinations of the following alleles or transgenes: *Lgr5*^{DTR-GFP} (Tian et al., 2011), *Atoh1*^{CreERT2} (Fujiyama et al., 2009), and *Tnf*^{fllox} (Grivennikov et al., 2005). All mice were between the ages of 14-20 weeks at the time of experiments.

Tissue preparation for mucin staining

For mucin staining, the ileum (distal third of small intestine) was isolated. Fragments of 1.5 cm length containing fecal pellets were then isolated and placed directly into methacarn fixative (60% methanol, 30% chloroform, 10% acetic acid). Fragments were fixed for 7 days rocking at room temperature. Following fixation, fragments were washed twice in methanol for 20 minutes each wash, twice in absolute ethanol for 20 minutes

each, and twice in xylene for 10 minutes each. The tissue was then embedded in paraffin blocks following standard procedures and cut into 4 μ m sections.

Immunofluorescence and immunohistochemistry

Methods were followed according to Chapter 2 of this dissertation.

Intestinal transit assay

Mice were fasted 24 hours prior to tissue harvest and given free access to water. Sterile saline solution (0.9% NaCl) was used to resuspend 70 kD FITC-Dextran (46945, Sigma) at a concentration of 25 mg/ml. Each mouse was administered 0.5 mg (20 μ l) of 70 kD FITC-Dextran solution by oral gavage for 1 hour. The gastrointestinal tract from stomach to rectum was then harvested and imaged on a BioRad ChemiDoc Touch Imaging System using a SYBR Green filter. Displacement of FITC was measured starting at the stomach-duodenum junction.

Bacterial load 16s rRNA qPCR

Fecal pellets were harvested from the ileum of mice and immediately stored at -20°C . Genomic DNA (gDNA) was later isolated using the Qiagen DNeasy PowerLyzer PowerSoil Kit following the manufacturer's protocol. qPCR targeting the universal bacterial 16s rRNA gene was then performed on isolated gDNA using universal 16s primers (33) and primers targeting mouse genomic GAPDH. Relative 16s copies were calculated using the $\Delta\Delta\text{Ct}$ method by normalizing 16s Ct values to mouse genomic GAPDH Ct values, similar to what has been reported (34).

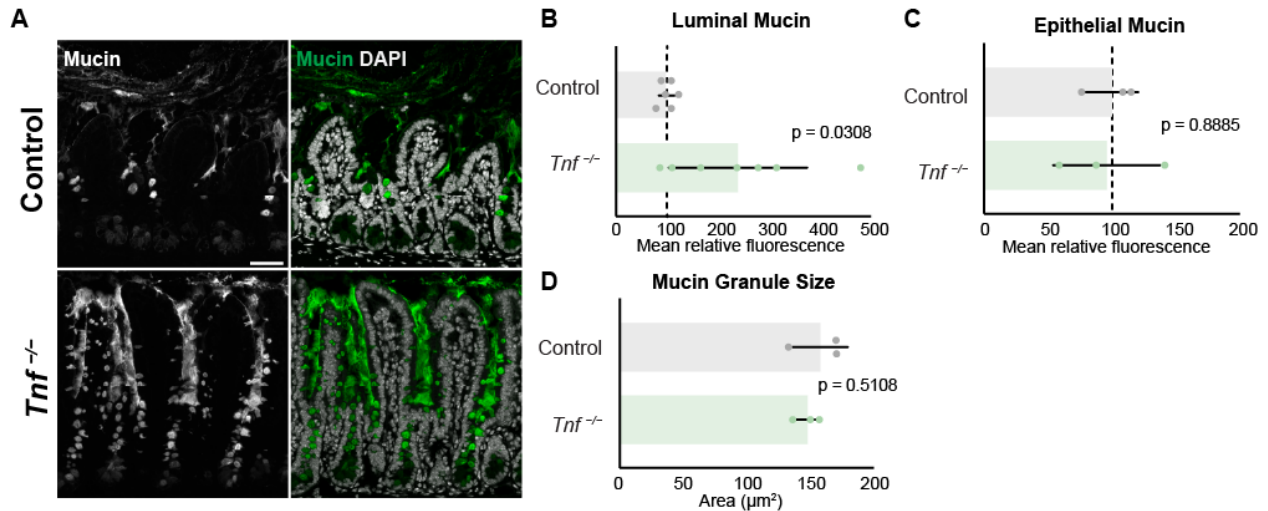


Figure 3.1. Global loss of *Tnf* leads to an increase in luminal mucin, but not cellular mucin. (A) Immunofluorescence of mucin by UEA-1 lectin stain in adult intestine. *Tnf*^{-/-} mice have stronger staining intensity and more luminal area covered by mucin. Scale Bar = 200 μm. (B) Quantification of mean fluorescence intensity of inter-villus regions. Values are normalized to mean fluorescence of controls, N = 6 mice per group, at least 15 regions of interest per mouse. (C) Quantification of Muc2 staining intensity per goblet cell. N=3 mice per experimental group. Mean represents all goblet cells in the distal 10 cm segment of a sectioned intestine. Values normalized to mean of control. (D) Granule size, the mean fluorescence area of Muc2 stain of the same regions of interest marked in panel C. p-value calculated by unpaired two-tailed t-test.

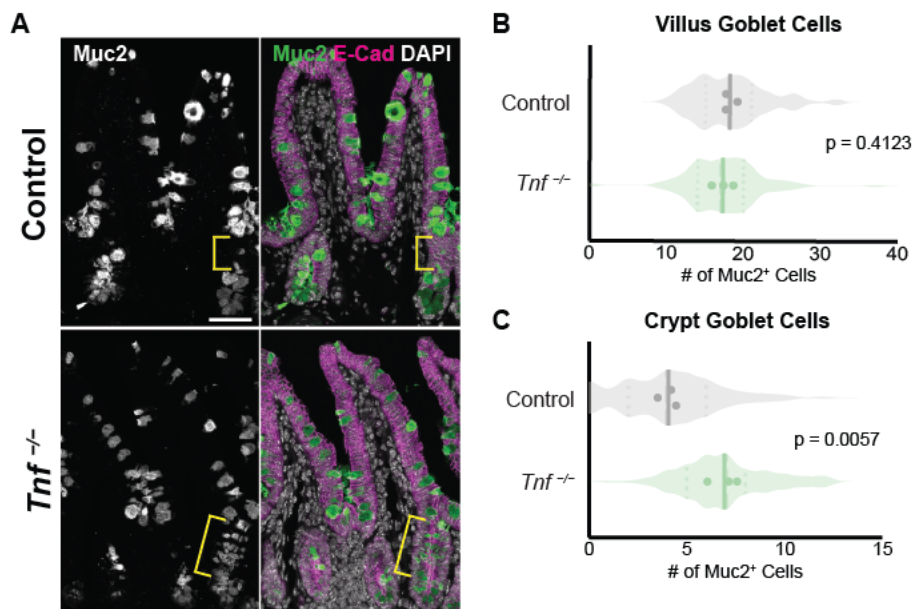


Figure 3.2. Absence of *Tnf* causes an increase in crypt goblet cell number. (A) Immunostaining of Muc2⁺ goblet cells. There is an increased number of goblet cells in *Tnf*^{-/-} intestines. Yellow brackets indicate Muc2⁺ goblet cells above Paneth cell zone in crypt. Scale Bar = 50 μm. (B,C) Quantification of goblet cells in crypts and villi of mice.

N=3 mice per group, at least 30 full profile crypt-villus units counted per mouse. p-value calculated by unpaired two-tailed t-test.

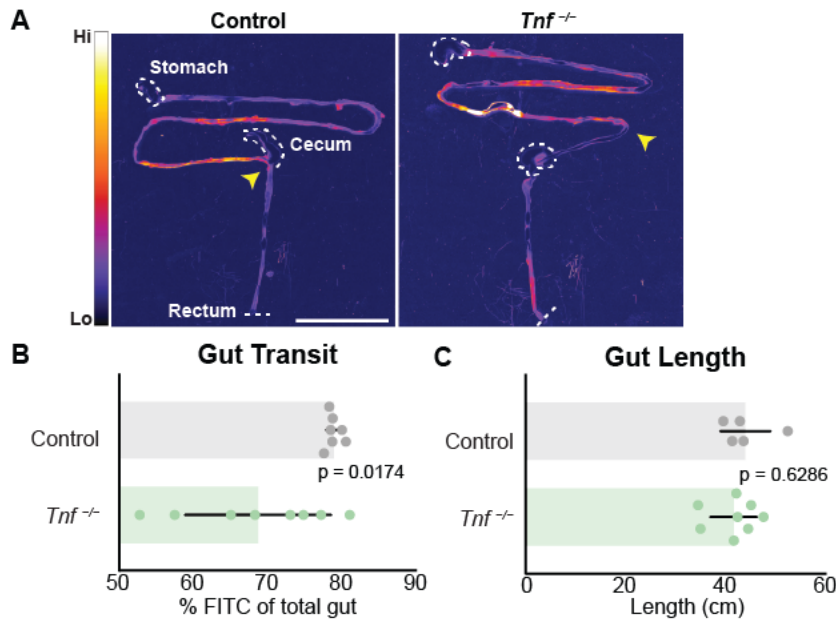


Figure 3.3. Loss of *Tnf* causes increased gut transit time. (A) Micrograph of full-length intestines showing FITC displacement after 1 h. Arrows indicate the most distal FITC signal. Dashed lines outline tissue landmarks. Scale Bar = 5 mm. (B) Quantification of FITC displacement represented as percent of gut length i.e. FITC signal over total gut length. N = 6 Control mice, N = 7 *Tnf*^{-/-} mice. (C) Total gut length is quantified as the distance from stomach to the rectum of mice. N = 5 Control mice, 8 *Tnf*^{-/-} mice. p-value calculated by unpaired two-tailed t-test.

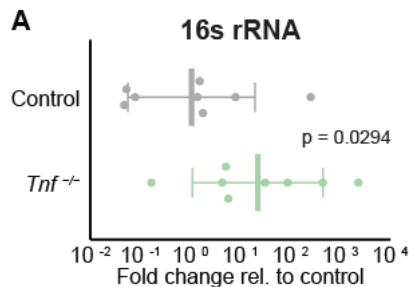


Figure 3.4. Absence of *Tnf* leads to increased bacterial load in the intestine. (A) Relative bacterial load in feces collected from the ileum of mice calculated based on fold change of 16s rRNA expression compared to control N = 8 mice per group. p-value calculated by unpaired one-tailed t-test.

Chapter 4: TNF does not affect secretory cell turn-over, but controls goblet cell number by regulating secretory progenitor cell differentiation

Goblet cell number depends on the rate of loss of mature goblet cells through mechanisms like cell death and extrusion from the villi and the rate of differentiation from secretory progenitors. We investigated how goblet cell numbers increase in the crypts of *Tnf*^{-/-} mice using a lineage tracing approach, focusing on the fate of secretory progenitors. We bred *Atoh1*^{CreERT2}; *Rosa26*^{tdTomato} mice (35–37), which label secretory progenitors upon tamoxifen induction, with *Tnf*^{-/-} mice, and then lineage traced secretory progenitors in the absence of TNF.

Crypt cells give rise to differentiated cells that displace more mature cells along the crypt-villus axis until the most distal cells ultimately die and are shed at the villus tips (37). This continuous epithelial turnover takes approximately 3-5 days in the small intestine (2, 32). We predicted that lower rates of differentiated cell turnover would lead to an increase in goblet cell number due to the persistence of differentiated goblet cells in the epithelium. To explore this possibility, we measured the displacement of labeled proliferating cells in *Atoh1*^{CreERT2}; *Rosa26*^{tdTomato}; *Tnf*^{-/-} mice as a proxy for secretory cell turnover (37, 39). We treated mutant mice with a single tamoxifen dose at day 0 and a single injection of the thymidine analog EdU at day 1 (Figure 4.1, A). Over the course of 3 days, proliferative secretory progenitors would be labeled with both tdTomato and EdU, enabling us to map the appearance of nascent mature secretory cells arising from secretory progenitors and to measure the displacement of double-positive tdTomato⁺/EdU⁺ cells up the villus. We found that control and mutant secretory progenitor cells alike were displaced ~ 50 μm from the hinge region that separates the crypt and villus compartments (Figure 4.2, A-B),

suggesting that secretory cell turnover was unaltered. Therefore, we next assessed the number of secretory progenitors in crypts, which would affect the overall rate of differentiation into goblet cells.

To label secretory progenitors while minimizing lineage tracing of differentiated secretory cells, we induced *Atoh1*^{CreERT2}; *Rosa26*^{tdTomato}; *Tnf*^{-/-} mice with a single tamoxifen pulse followed by a short chase of 36 hours (Figure 4.1, A). Labeled *Atoh1*^{CreERT2}; *Rosa26*^{tdTomato}; *Tnf*^{-/-} mice had increased numbers of tdTomato⁺ cells within crypts, indicative of a secretory differentiation bias (Figure 4.3, A). Since the crypt houses secretory (ATOH1⁺) and absorptive (NICD⁺) progenitors (36), we next assessed if the increase in ATOH1⁺/tdTomato⁺ secretory progenitors was specific to this lineage and did not include an increase in absorptive progenitors, by staining absorptive progenitors for NICD (Figure 4.4, A). We found that *Tnf*^{-/-} mice have a disproportionate increase in tdTomato⁺ secretory progenitors with a corresponding decrease in absorptive progenitors (Figure 4.4, B-C). The total number of progenitors per crypt increased (Figure 4.4, D) and crypt length was unchanged (Figure 4.4, E), indicating that there was a biased increase in secretory progenitors.

METHODS

Tamoxifen induction

Tamoxifen (T5648-5g, Sigma) was dissolved in corn oil and administered via oral gavage at a dosing of 1mg tamoxifen/kg of body weight for each mouse. To label secretory progenitors, mice were given a single dose of tamoxifen at the start of the experiment, and tissue was harvested at either 36 hours or 72 hours post-induction.

All tissue was prepared and imaged as outlined in Chapter 2.

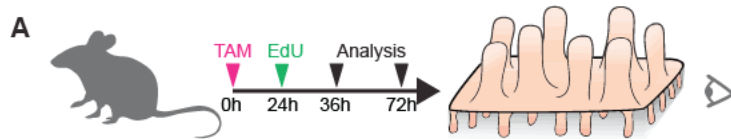


Figure 4.1. Experimental design. (A) *Atoh1^{CreERT2}; Rosa26^{tdTomato}* Control and *Tnf^{-/-}* mice induced with tamoxifen at 0 h to label secretory progenitors, injected with EdU at 24 h to label proliferating cells, and analyzed at 36 h and 72 h.

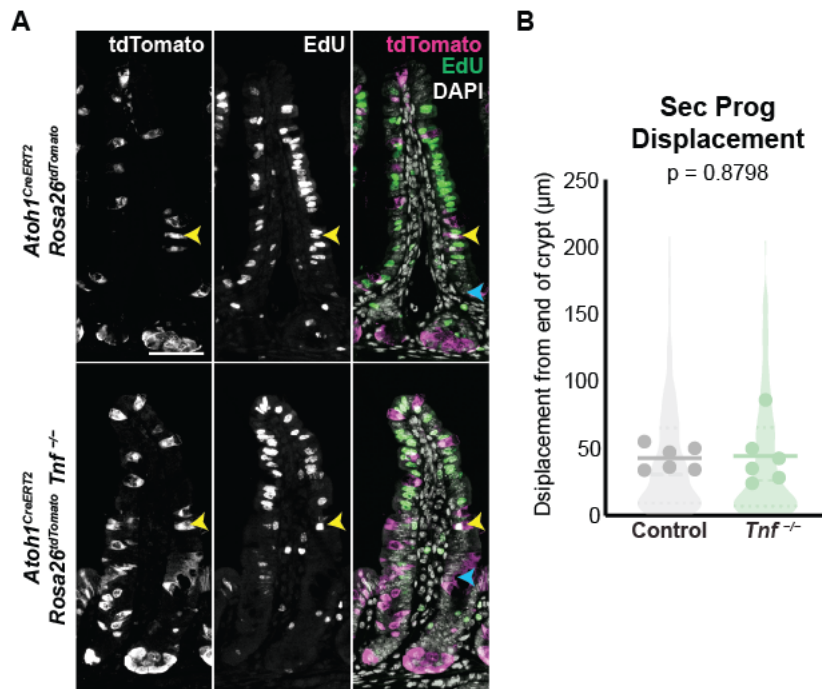


Figure 4.2. Secretory progenitor cell displacement after 48 h is unaffected in *Tnf^{-/-}* mice. (A) Micrograph of *Atoh1^{CreERT2}; Rosa26^{tdTomato}* Control and *Tnf^{-/-}* mice after labeling of proliferating secretory progenitor cells at 24 h and a 48 h chase. (B) The displacement of secretory progenitor daughters (tdTomato* EdU* cells) from the hinge region was measured and quantified. N = 6 mice per group, at least 25 full profile crypt-villus units were measured per mouse. p-value calculated by unpaired two-tailed t-test.

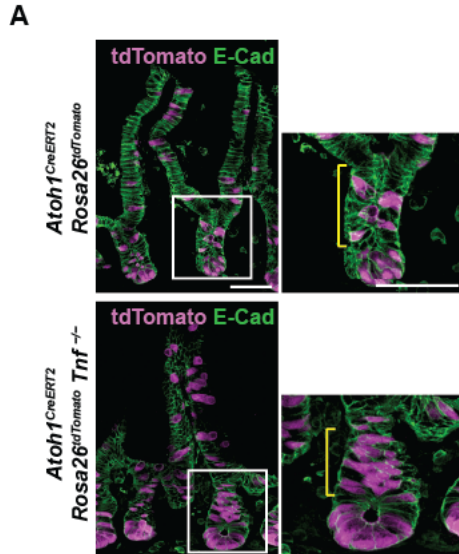


Figure 4.3. Loss of *Tnf* results in an increase in secretory progenitors.
 (A) Micrograph of *Atoh1^{CreERT2}; Rosa26^{tdTomato}* Control and *Tnf^{-/-}* mice induced with tamoxifen for 36 h to label secretory progenitors. Scale bar = 50 μ m. White boxes highlight insets. Yellow brackets show the progenitor zone.

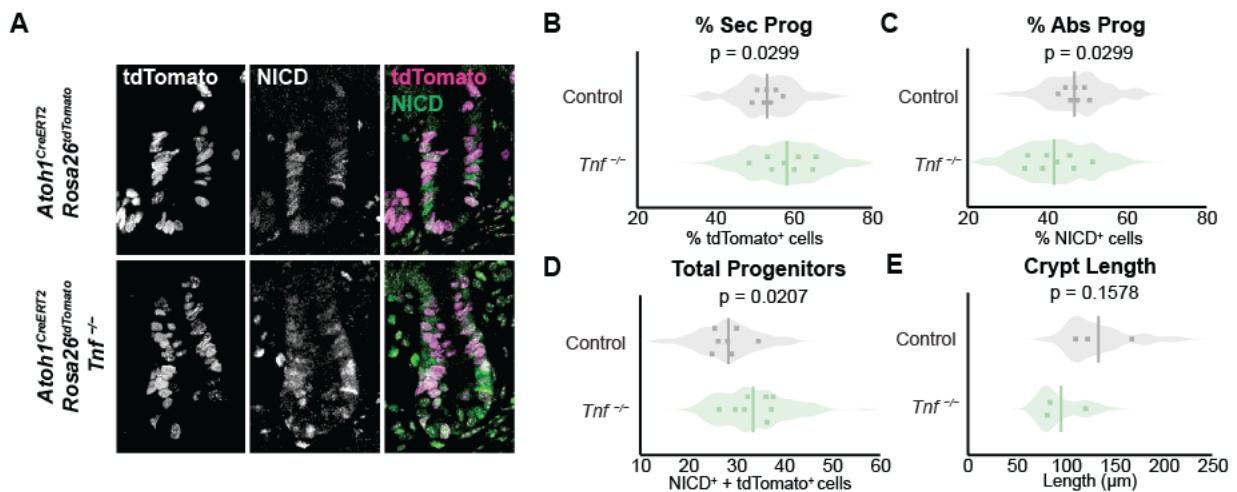


Figure 4.4. Secretory progenitors increase at the expense of absorptive progenitors upon loss of *Tnf*. (A) Representative crypts labeled for both absorptive (NICD⁺) and secretory (tdTomato⁺) progenitors. Scale bar = 50 μ m. (B) Percent secretory progenitors was quantified as the number of (tdTomato⁺) cells over total progenitors (NICD⁺ and tdTomato⁺). N = 7 Control mice, 8 *Tnf^{-/-}* mice, at least 20 full profile crypts per mouse. (C) Percent absorptive progenitors was quantified as the number of (NICD⁺) cells over total progenitors (NICD⁺ and tdTomato⁺). N = 7 Control mice, 8 *Tnf^{-/-}* mice, at least 20 full profile crypts per mouse. (D) The number of progenitor cells was quantified as the number of NICD⁺ and tdTomato⁺ cells from the +4 region to the top of the crypt. N = 7 Control mice, 8 *Tnf^{-/-}* mice, at least 20 full profile crypts per mouse. (E) Crypt length was measured as the distance from the bottom of the crypt to the hinge region. N = 3 mice per group, at least 30 full profile crypts were measured per mouse. p-value calculated by unpaired two-tailed t-test.

Chapter 5: Epithelial-derived TNF is required for mucin and goblet cell homeostasis

Immunohistochemical analysis of TNF confirmed that Paneth cells are the major epithelial source of TNF (Figure 2.2, A)(26, 27), but also indicated the presence of numerous TNF⁺ cells in the subepithelial mesenchyme, raising the question of whether epithelial- as opposed to stromal-derived TNF plays the central role in mucin homeostasis. Using mice harboring both the *Vil^{CreERT2}* and *Tnf^{flx/flx}* alleles (40, 41) we deleted TNF in intestinal epithelial cells with daily doses of tamoxifen over 6 days, which is ~ 2 epithelial turnover cycles (Figure 5.1, A). We then stained for luminal mucin and goblet cell numbers and compared results to major phenotypes seen in global TNF knockout mice. Acute epithelial loss of TNF reproduced the defects observed during constitutive global loss of TNF. While mutants showed no difference in gut length compared to controls (Figure S5.1, A-C), they had increased luminal mucin (Figure 5.2, A-B). We also observed higher goblet cell numbers (Figure 5.3, A and C) in the crypt (Figure 5.3, C), while villus (Figure 5.3, B) and total goblet cell numbers remained unchanged (Figure S5.2, A). To determine whether acute epithelial loss of TNF also caused defects in waste expulsion, we performed a gut transit assay. After 6 days of tamoxifen induction, we measured the distance that FITC-Dextran traveled along the gastrointestinal tract over 1 h. The dye traveled 6% less of the total gut in mutant mice compared to controls (Figure 5.4, A-B), similar to what we observed in *Tnf^{-/-}* mice. Taken together, our studies establish a central role for epithelial-derived TNF in regulating mucin homeostasis by inhibiting secretory progenitor bias to goblet cells.

METHODS

Tamoxifen induction

Tamoxifen (T5648-5g, Sigma) was dissolved in corn oil and administered via oral gavage at a dosing of 1mg tamoxifen/kg of body weight for each mouse. For conditional knock-out studies, mice were given a single dose of tamoxifen each day by oral gavage for 6 consecutive days.

All tissue was prepared. Immunostained, and imaged as outlined in Chapter 2.

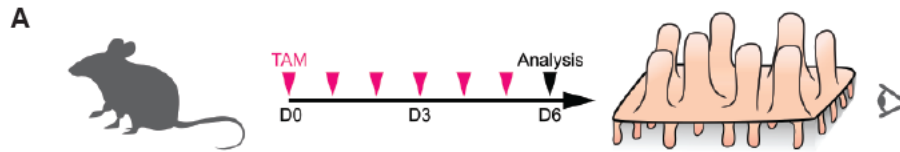


Figure 5.1. Experimental design. (A) *Villin^{CreER}; Tnf^{flox/flox}* mice and control mice were given a single dose of tamoxifen each day by oral gavage for 6 consecutive days.

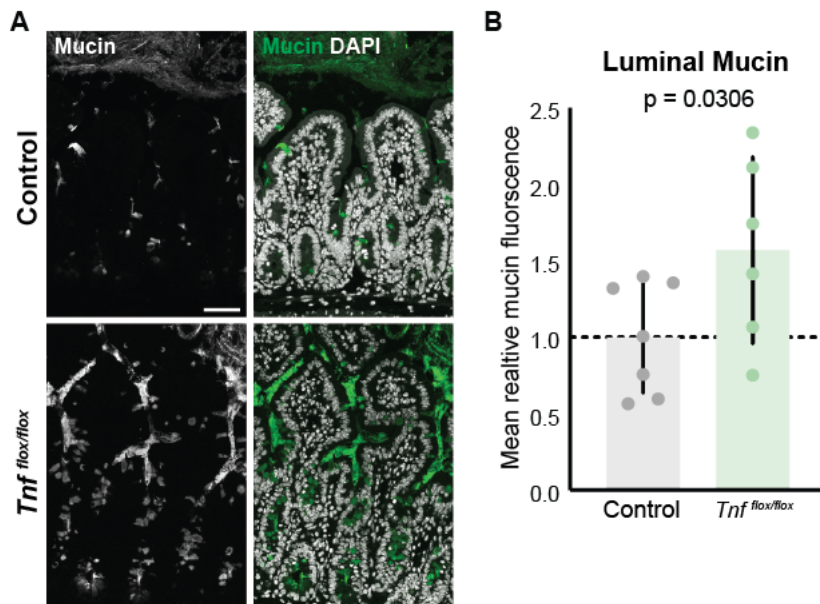


Figure 5.2. Intestinal epithelial-specific ablation of *Tnf* reproduces luminal mucin defects seen in global ablation studies. (A) Immunofluorescence of mucin by UEA-1 lectin stain in adult tissue. Note that *Villin^{CreER}; Tnf^{flox/flox}* mice have stronger staining intensity and more luminal area covered by mucin. Scale bar = 50 μ m. (B) Quantification of mean fluorescence intensity of inter-villus regions. Values are normalized to mean fluorescence of controls. N = 6 Control mice, 7 *Villin^{CreER}; Tnf^{flox/flox}* mice. At least 20 ROIs per mouse were counted. p-value calculated by two-tailed t-test.

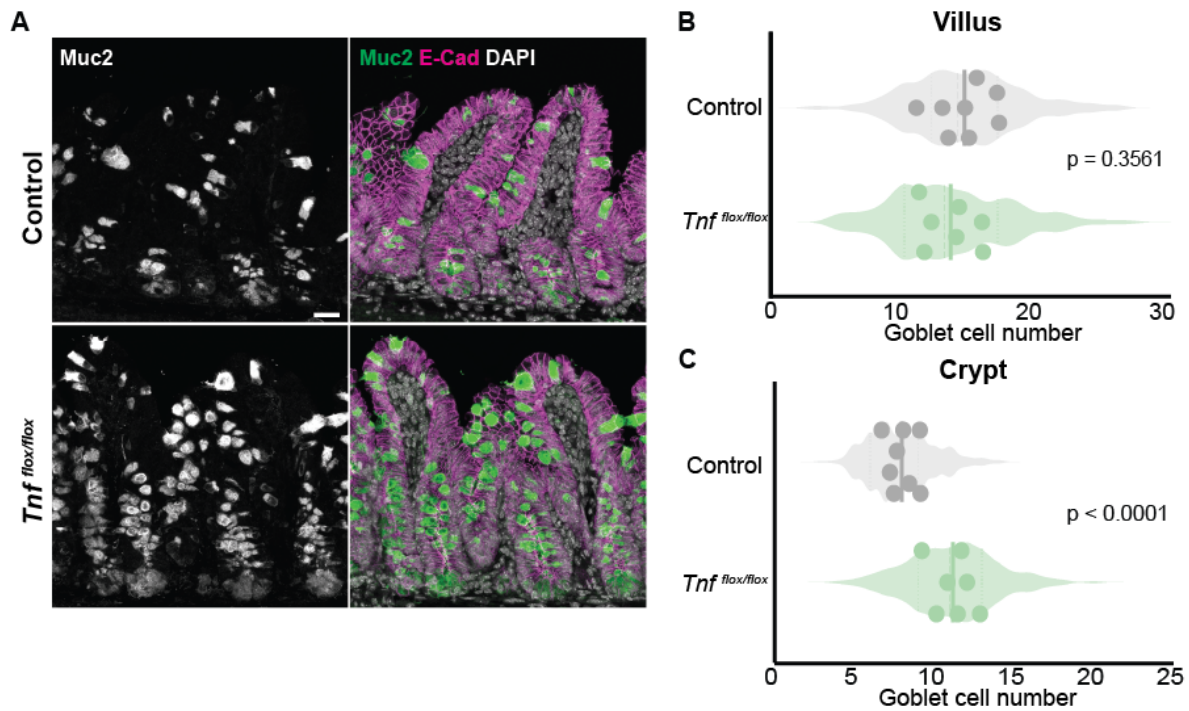


Figure 5.3. Loss of epithelial TNF leads to an increase in crypt goblet cells. (A) Micrograph of Muc2⁺ goblet cells in the intestine. Scale bar = 50 μ m. (B, C) Quantification of Muc2⁺ goblet cells. N = 5 Control mice, 6 *Villin*^{CreER}; *Tnf*^{flx/flx} mice. At least 25 crypt-villus units per mouse were counted. p-value calculated by two-tailed t-test.

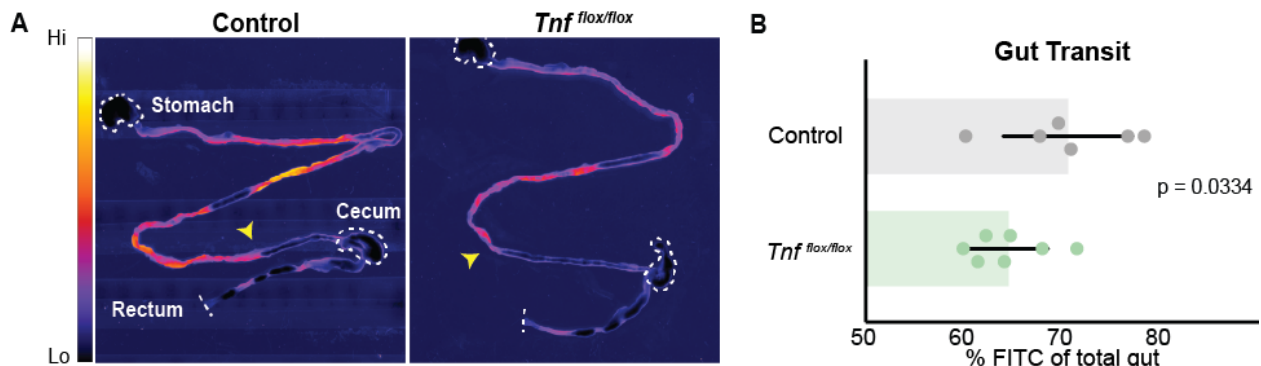


Figure 5.4. Loss of epithelial TNF results in slower gut transit. (A) Micrograph of FITC displacement after 1 h across full-length intestines. Arrows indicate most distal FITC signal. Dotted lines outline tissue landmarks. Scale Bar = 2 mm. (B) Quantification of FITC displacement represented as percent of gut length, i.e. FITC signal over total gut length. N = 6 Control mice, 7 *Villin*^{CreER}; *Tnf*^{flx/flx} mice.

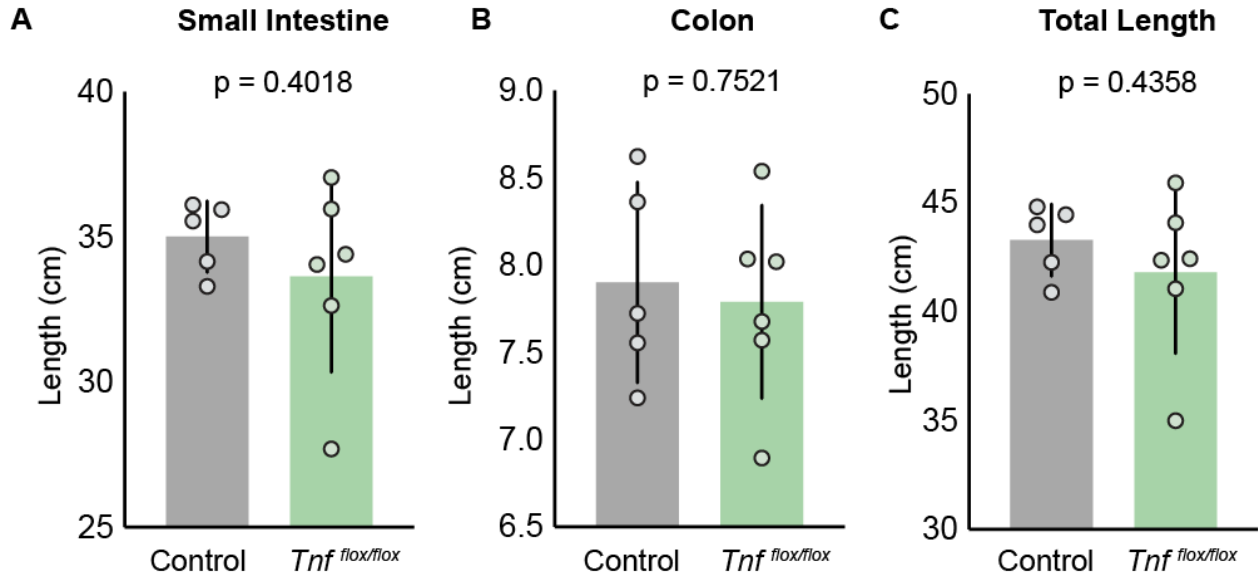


Figure S5.1. *Villin*^{CreERT2}; *Tnf*^{flox/flox} mice show no defects in intestine length. (A-C) Full-length intestine (stomach to rectum) was isolated, photographed, and digitally measured. (A) The small intestine was defined as the segment starting from the end of the stomach to the beginning of the cecum. (B) The colon was defined as the segment starting after the cecum and ending at the rectum. (C) Total length was defined as the entire isolated segment (stomach to rectum). p-value calculated by unpaired two-tailed t-test for panels A-C.

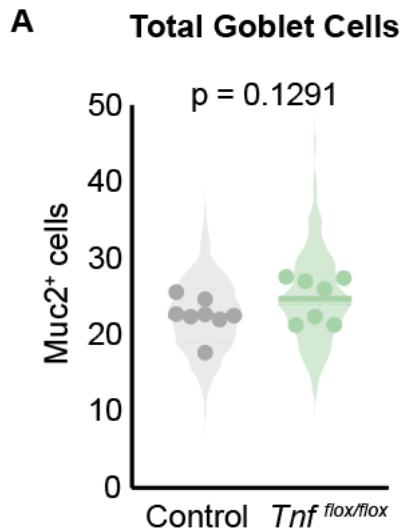


Figure S5.2. *Villin*^{CreERT2}; *Tnf*^{flox/flox} mice maintain total goblet cell number. (A) Quantification of Muc2⁺ goblet cells. N = 5 Control mice, 6 *Villin*^{CreER}; *Tnf*^{flox/flox} mice. At least 25 crypt-villus units per mouse were counted. p-value calculated by unpaired two-tailed t-test for panel A.

Chapter 6: Epithelial-derived TNF modulates CFTR induced fluid pumping and Meprin- β shedding, which are required for proper mucin flux

Several phenotypes observed in our *Tnf*^{-/-} mice resembled those previously reported in *Cftr*^{-/-} mice, including increased intestinal mucin levels, goblet cell number, gut transit, and bacterial load (9, 10, 32). CFTR function is essential for proper mucin flux and maturation in the intestine (11, 12), so we asked if epithelial TNF acted as an upstream regulator in addition to regulating the proportion of secretory progenitors. We first characterized the spatial expression of CFTR within the intestine using RNAscope and found that *Cftr* transcripts were spatially restricted to epithelial crypts in the ileum, and that at the crypt base LGR5⁺ stem cells highly expressed *Cftr* (Figure 6.1, A). These data suggest that the crypt base is a major site of fluid and ion pumping downstream of CFTR. Furthermore, the zoned expression of CFTR, TNF ligand (Figure 2), and TNF receptors (Figure 2) at epithelial crypts suggest potential interactions between CFTR and TNF in the intestine.

Intestinal organoids provide an ideal system to dissect molecular mechanisms intrinsic to the epithelium by enabling genetic and pharmacological perturbation studies in a dish. During normal organoid growth, fluid flows into organoid lumens and causes them to periodically inflate and collapse in a CFTR-dependent manner (42). Indeed, inflation of organoids has been used to predict patient response to drugs in cystic fibrosis, which is caused by loss-of-function mutations in CFTR (43, 44). We assessed the impact of TNF on CFTR activity by first measuring the rates of inflation of control and *Tnf*^{-/-} organoids cultured in normal growth conditions. By qPCR analysis of 1-day old control and *Tnf*^{-/-} organoids, we found no change in *Cftr* expression (Figure 6.1, B), suggesting that any

effects on inflation would be post-transcriptional. The rate of inflation of *Tnf*^{-/-} organoids was significantly reduced in normal growth media, ~ 2.5 times slower than controls (Figure 6.2, A-B). Consistent with a role for TNF upstream of CFTR, recombinant TNF rescued the lumen size of *Tnf*^{-/-} organoids at 24 h of growth, and combined treatment with rTNF and the CFTR inhibitor CFTRinh-172 blocked the previously observed rescue (Figure 6.2, C).

We hypothesized that rTNF was increasing the functional pool of CFTR in organoids. To get a more accurate read out of maximum CFTR function we used forskolin to elevate cyclic AMP levels and stimulate CFTR activity and swelling in intestinal organoids (43). Previous work showed that rTNF stimulates CFTR activity through a PKC-dependent mechanism in human bronchial epithelial cells (45). Therefore, we co-stimulated wild-type organoids with forskolin and combinations of rTNF, CFTR-inh172, and the PKC inhibitor Bisindolylmaleimide I (GF109203X). We found that TNF had an additive effect with forskolin in inducing organoid swelling and caused an overall 2-fold increase in lumen swelling. This additive effect was abrogated with CFTR inhibition, confirming that rTNF-induced swelling acts through CFTR. Additionally, rTNF co-treatment with the PKC inhibitor GF109203X abrogated the additive effect of rTNF, pointing to a PKC-dependent mechanism (Figure 6.3, A-B). Thus, rTNF modulates CFTR-induced fluid pumping through PKC.

CFTR and the protease Meprin- β both contribute to proper mucin homeostasis. Ions released by CFTR promote mucin unfolding, which exposes sites that Meprin- β can then cleave allowing mucin to be processed and released (5). Mucin can only be cleaved by the protease Meprin- β once it is shed from the cell surface and is in its soluble form.

Failure to shed Meprin- β from epithelial cell membranes leads to unprocessed MUC2 and more dense mucus (12).

Finally, we asked whether epithelial TNF also acts upstream of Meprin- β and assessed the activity of Meprin- β in *Vil*^{CreERT2}; *Tnf*^{flox/flox} mice by using protease localization as a readout. We deleted epithelial *Tnf* with daily doses of tamoxifen over 6 days in *Vil*^{CreERT2}; *Tnf*^{flox/flox} mice and measured the amount of Meprin- β at the cell membrane by immunostaining (12). *Vil*^{CreERT2}; *Tnf*^{flox/flox} mice showed more intense and dense Meprin- β staining compared to controls indicative of less shed Meprin- β and consequently a decreased ability to cleave mucin (Figure 6.4, A). These results expand the role of epithelial TNF in mucin homeostasis beyond control of goblet cell number to include modulation of two key processes in mucin flux: regulation of CFTR activity and Meprin- β shedding.

METHODS

Small molecules and recombinant proteins

Mouse recombinant TNF α (410-MT-025/CF, R&D Systems) was resuspended in PBS with 0.1% BSA at a concentration of 100 μ g/ml and stored at -80 °C. CFTR-inh172 (C2992, Millipore Sigma) was resuspended in DMSO at a concentration of 50 mM and stored at -80 °C. Forskolin (Sigma 6886-10MG) was resuspended in DMSO at a concentration of 50 mM and stored at -80 °C. Bisindolylmaleimide I (GF109203X) was resuspended in DMSO at a concentration of 10 mM and stored at -80 °C. EGF (53003-018, Invitrogen) was resuspended in PBS with 0.1% BSA at a concentration of 50 μ g/ml

and stored at $-20\text{ }^{\circ}\text{C}$. Noggin (6057-NG-100/CF, R&D Systems) was resuspended in PBS with 0.1% BSA at a concentration of $100\text{ }\mu\text{g/ml}$ and stored at $-20\text{ }^{\circ}\text{C}$. Y-27632 (125410, Tocris) was resuspended in DMSO at a concentration of 10 mM and stored at $-20\text{ }^{\circ}\text{C}$. Jagged Chimera (AS-61298, Anaspec) was resuspended in sterile MilliQ H_2O at a concentration of 1 mM and stored at $-20\text{ }^{\circ}\text{C}$.

Organoid tissue culture

Mouse intestinal organoid cultures were established from ileal segments isolated from mice aged 12-20 weeks, according to established protocols (46). Briefly, following 15 minutes of incubation in intestine harvest buffer, fileted intestinal segments were placed in crypt dissociation buffer and rocked on ice for 1 hour. Crypts were filtered through a $70\text{ }\mu\text{m}$ mesh filter. Crypts were plated in a pre-heated 24 well plate in Matrigel (356231, Corning) supplemented with 10% R-Spondin conditioned medium, Jagged Chimera ($10\text{ }\mu\text{M}$), Noggin (100 ng/ml), and EGF (50 ng/ml). After Matrigel droplets solidified, organoids were overlaid with $500\text{ }\mu\text{l}$ ENR medium supplemented with Y-27632 ($10\text{ }\mu\text{M}$). After 48 hours, medium was changed to ENR medium alone. From this point forward, organoids were cultured in standard ENR.

Live imaging of organoids

Ileal organoids were passaged at day 7 in culture by mechanical dissociation and plated in a 96-well plate format. Organoids were plated at a density of 50 organoids per every $3\text{ }\mu\text{l}$ droplet of Matrigel. After the droplet solidified, each well was overlaid with $200\text{ }\mu\text{l}$ ENR medium supplemented with the appropriate drug treatments. The plate was

immediately transferred to a Zeiss Cell Observer spinning disc confocal system with Yokogawa CSU-X1M and incubation chamber. The system was pre-equilibrated for 30 minutes to 37 °C and 5% CO₂. Images were acquired every 20 minutes for 48 hours, at 5x magnification using brightfield trans-luminescence. A 90 µm z-stack was taken per region (z-step = 30 µm).

Forskolin-induced swelling assay

Organoids were passaged into a 96-well plate at a density of 50 organoids per well and allowed to grow in normal ENR media for 2 days. At the start of the experiment, old media was replaced with 100 µl of fresh media containing 1 ng/ml rTNF, 20 µM CFTR-inh172, and 5 µM GF109203X. The plate was then placed back in the incubator for 4 h at 37°C 5% CO₂. Afterward, 100 µl of media containing additives plus 0.8 µM forskolin was quickly added to wells to give a total well volume of 200 µl and a final concentration of 0.4 µM forskolin. The plate was immediately transferred to a Zeiss Cell Observer spinning disc confocal system with Yokogawa CSU-X1M and incubation chamber. The system was pre-equilibrated for 30 minutes to 37 °C and 5% CO₂. Tiled images of the center plane of each well were acquired every 10 m for 120 m at 5 x magnification.

All mouse intestine tissue was prepared, Immunostained, and imaged as outlined in Chapter 2.

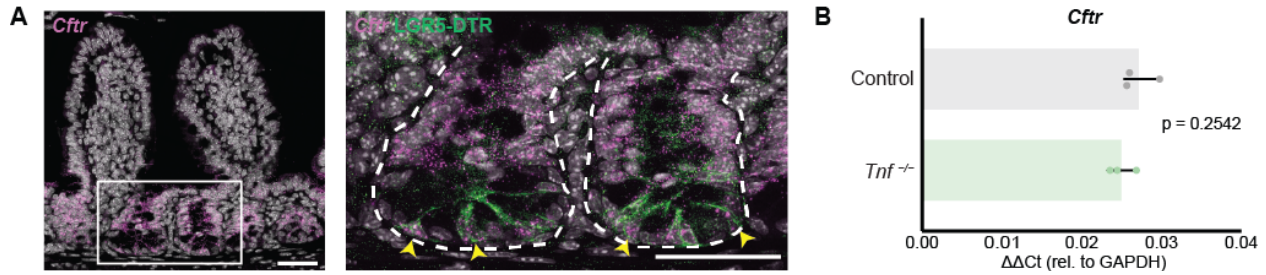


Figure 6.1. *Cftr* is expressed in mouse epithelial crypts and intestinal organoids. (A) RNAscope of *Cftr* and immunofluorescence staining of LGR5-DTR mouse intestine. Scale Bar = 50 μ m. White box outlines inset. Dotted line marks epithelial-mesenchymal broder. N = 3 LGR5-DTR mice. Yellow arrows mark LGR5⁺ stem cells with high *Cftr* expression. (B) qPCR analysis of *Cftr* expression in day 1 organoids. N = 3 distinct organoid lines per group.

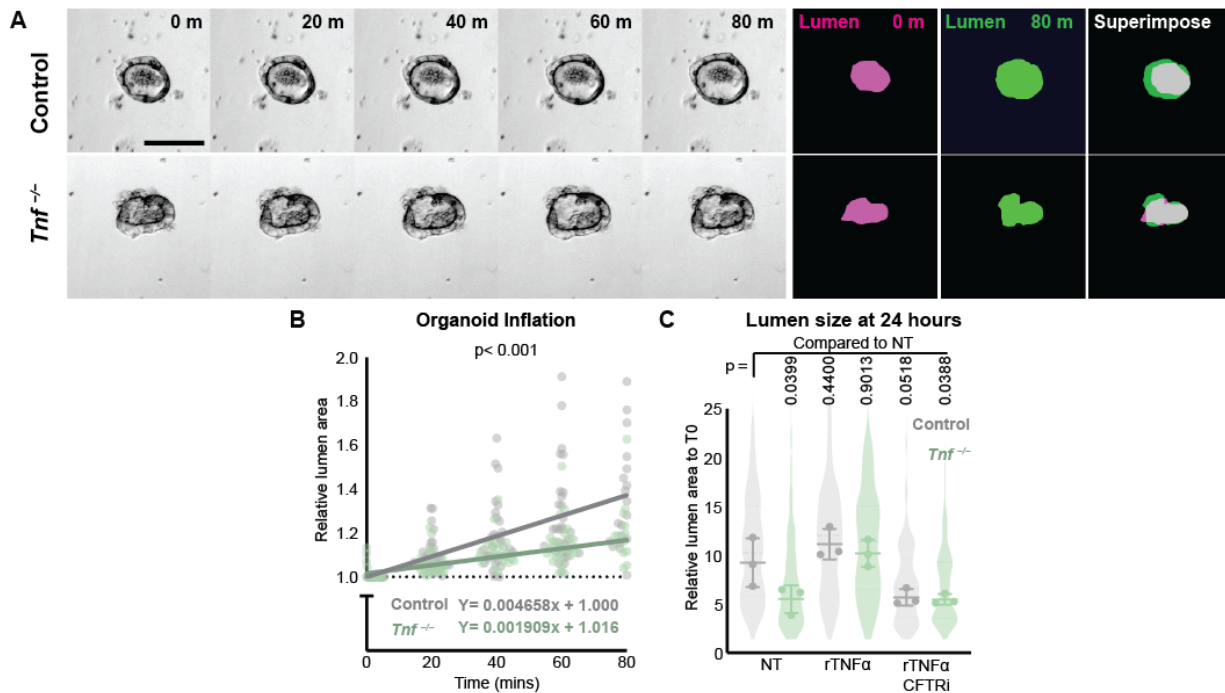


Figure 6.2. TNF promotes intestinal organoid fluid pumping via CFTR. (A) 80 m montage of WT and *Tnf*^{-/-} organoids live imaged 8 h after plating under normal growth conditions. Magenta masks outline lumens at 0 m and green masks outline lumens at 80 m. Scale bar = 50 μ m. N = 3 distinct organoid lines per group. (B) Quantification of the rate of inflation of organoids during 80 m without lumen collapse under normal growth conditions. Lumen size was normalized to t = 0 and was measured for each individual organoid at 20 m intervals. A simple linear regression was performed for compiled data. N = 3 distinct organoid lines per group. 30 organoids total per group were analyzed. (C) Lumen size of organoids treated with 1 ng/ml rTNF and 50 μ M CFTRinh-172 for 24 h. Measurements were normalized to the size of individual lumens at t = 0 h. N = 3 distinct organoid lines per group. 25 organoids per organoid line were quantified. A two-tailed p-value was calculated testing the null hypothesis that the

slopes between the two groups were equal in panel B. A p-value was calculated using an ordinary one-way ANOVA analysis with Dunnet's multiple comparison's test comparing all groups to the control for panel C.

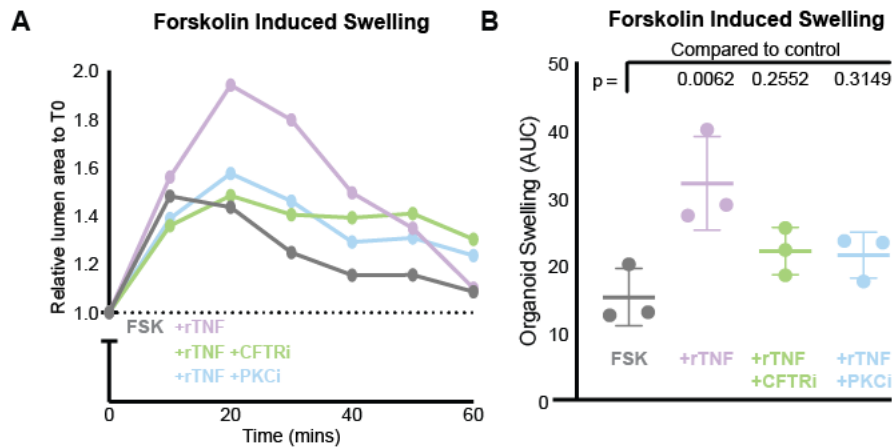


Figure 6.3. rTNF treatment of organoids modulates forskolin induced swelling in a PKC dependent manner. (A) Lumen swelling of 2 day old wild type organoids co-stimulated with 0.4 μ M FSK and 1 g/ml rTNF plus inhibitors of either CFTR (20 μ M CFTRinh-172) or PKC (5 μ M GF 109203X). Plots represent mean of 30 organoids from 3 distinct organoid lines. Inset highlights increased swelling in rTF treated groups. (B) Area under the curve of forskolin induced swelling plots. Each point represents the mean AUC for an individual organoid line within the group. p-value was calculated using an ordinary one-way ANOVA analysis with Dunnet's multiple comparison's test comparing all groups to the control.

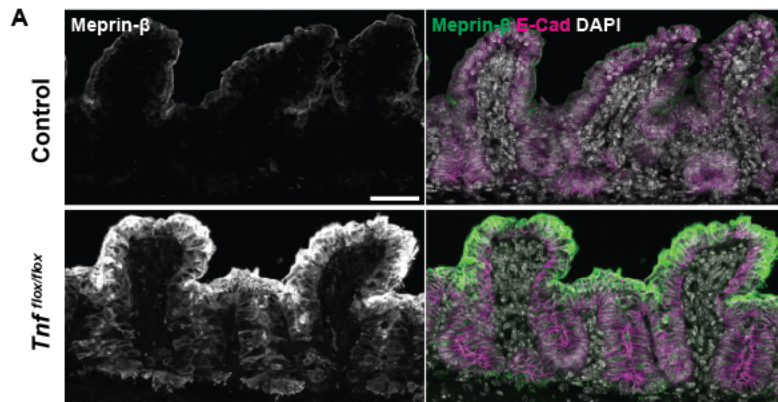


Figure 6.4. Epithelial TNF regulates Meprin- β shedding. (A) Immunofluorescence of Meprin- β in the intestine. N = 6 Control mice, 7 *Villin^{CreER}; Tnf^{flox/flox}* mice.

Chapter 7: Discussion

Mucin provides a layer of protection against external pathogens and contaminants (5, 6). In the respiratory tract, the epithelium is kept free of pathogens by active ciliary movement that clears mucin away from the epithelium. In contrast, the digestive tract lacks ciliary movement but still maintains flux of mucin away from the epithelium (5). In healthy intestines, the mucus layer facilitates waste expulsion, protects the host against pathogens, and houses commensal microbes that aid in nutrient absorption (2, 47). However, in disease states mucus can accumulate in tissues, leading to increased bacterial load, inflammation, and tissue damage. Loss of the mucosal barrier can also lead to disease by induction of persistent intestinal inflammation, as seen in inflammatory bowel disease (IBD) (48). Thus, a balance between the maintenance and turnover of mucus is essential for tissue homeostasis. However, the upstream molecular mechanisms regulating the production and flux of mucin are poorly understood.

While TNF is a well-known inflammatory cytokine, we revealed previously underappreciated functions of TNF in epithelial mucin homeostasis. First, TNF regulates mucin production through its role in regulating differentiation of goblet cells, the mucin-producing cells in the respiratory and digestive tracts. Second, TNF controls the flux of mucin along the epithelial surface by inducing activity of the chloride channel CFTR and shedding of the protease Meprin- β . These newly identified roles expand our understanding of the functional repertoire of TNF.

Prior studies have focused on the impact of elevated levels of TNF on disease phenotypes (17, 20), overlooking its homeostatic role. The comprehensive analysis of TNF ligand-receptor expression in the intestinal epithelium presented here identified

Paneth cells as a primary source of TNF in the crypt epithelium. We propose that Paneth cell-derived TNF could establish a concentration gradient along the crypt-villus axis, similar to what has been proposed for AMPs secreted by Paneth cells (49). In other systems, cell geometry (50), ligand concentration (51), signal duration (52), and membrane organization (53) have all been shown to contribute to different cellular responses to TNF. Therefore, we propose that ligand gradient concentration, coupled with differential expression and localization of its receptors in the epithelium, may elicit different signaling responses to TNF in the intestine. In support of this idea, knocking down TNFR1 in the intestinal epithelium has different effects at the villus tip, lower villus, and crypt. For example, while reducing TNFR1 expression by 50% protects against Paneth cell or goblet dysfunction caused by exogenous TNF (54), it does not protect against villus tip cell death (55). However, complete knockout of TNFR1 does prevent cell death at the villus tip caused by exogenous TNF (55).

Developmental and *in vitro* studies have shown that TNFR2 signaling promotes transcription of *Muc2* (15, 19). In contrast to these studies, our work in adult mice found that TNF does not affect MUC2 protein expression but rather suppresses goblet cell differentiation. Expression analysis revealed that both TNFR1 and TNFR2 are enriched in the adult crypt, where stem cells and progenitors are localized. We also observed increased numbers of secretory progenitors and goblet cells specifically in the crypt epithelium when TNF is lost. Taken together, these data indicate that TNF signaling functions as a regulator of goblet cell differentiation in the crypt.

A number of studies have described TNF as a pro-differentiation factor of immune cells (56), skeletal muscle cells (57), and bone cells (58). Furthermore, NF- κ B, which is a

downstream effector of TNF signaling, is important for the Paneth vs. goblet cell fate decision. Genetic ablation of NF- κ B signaling in the intestine leads to a significant decrease in Paneth cell numbers, defective Paneth cell maturation, and increase in goblet cell number (59). We identified TNF as a differentiation factor in the intestine that has no effect on Paneth cell number but does control goblet cell number. This suggests that TNF may be acting independently of NF- κ B or on tangential signaling pathways in addition to NF- κ B. It will be important as a next step to determine if TNF derived from Paneth cells is the previously unidentified activator of homeostatic NF- κ B signaling in the intestine (59).

Our observation that TNF controls goblet cell number is supported by the work of several groups. Mouse studies have shown that TNF promotes the loss of goblet cells (17, 20, 60), while clinical studies of IBD patient samples, which typically have elevated TNF levels, also revealed a lower number of goblet cells and partial loss of mucus barriers (30, 61). Consistent with these findings, anti-TNF therapy in mouse colitis models causes goblet cell hyperplasia (62). Reduced goblet cell numbers in the context of elevated TNF have typically been interpreted as elevated goblet cell death. However, a recent RNAseq analysis of IBD colon patient samples with elevated TNF (63) revealed that there is also a decrease in secretory TA cells and immature goblet cells. Similarly, we found an increase in secretory progenitors at the expense of absorptive progenitors after the loss of TNF, accompanied by an increase in goblet cell number. Additionally, secretory lineage tracing and EdU pulse-chase experiments demonstrated no change in secretory cell turnover in the absence of TNF. These data suggest that TNF controls goblet cell numbers by regulating differentiation rather than cell death alone.

In organoids, we discovered that the pleiotropic effects of TNF on mucin homeostasis include induction of CFTR channel activity and flow, resulting in inflation of organoid lumens. TNF regulates the CFTR-dependent inflation-collapse dynamics observed in organoids, which is an important contributor to organoid cell patterning and morphogenesis (64). A more general link between TNF and CFTR is suggested by studies of human bronchial epithelial and HeLa cell monolayer cultures, in which TNF promotes CFTR apical localization and boosts cell chloride currents (45). Our studies are consistent with this body of work, suggesting a general mechanism of TNF modulation of CFTR activity across various tissues, including the intestine. Interestingly, pathologies associated with TNF or CFTR dysfunction exhibit several phenotypic similarities. For example, patients with cystic fibrosis are 7 times more likely to have IBD, a disease characterized by elevated levels of TNF (65). Additionally, CFTR knock-out mice exhibit increased mucin, slower gut transit, and increased bacterial load (10, 32), which align with our observations in the global and epithelial TNF loss of function experiments.

In conclusion, our data demonstrate that epithelial TNF is an essential regulator of mucin production and flux in the intestine. In addition to the canonical functions of TNF in inflammation and cell death, we reveal new roles for TNF in intestinal cell differentiation and modulation of CFTR activity.

References

1. Barker N. Adult intestinal stem cells: critical drivers of epithelial homeostasis and regeneration. *Nat. Rev. Mol. Cell Biol.* 2013;15(1):19–33.
2. Grondin JA, et al. Mucins in Intestinal Mucosal Defense and Inflammation: Learning From Clinical and Experimental Studies. *Front. Immunol.* 2020;11:2054.
3. Barker N, et al. Identification of stem cells in small intestine and colon by marker gene Lgr5. *Nat.* 2007 4497165 2007;449(7165):1003–1007.
4. Bonis V, Rossell C, Gehart H. The Intestinal Epithelium – Fluid Fate and Rigid Structure From Crypt Bottom to Villus Tip. *Front. Cell Dev. Biol.* 2021;9:1222.
5. Hansson GC. Mucus and mucins in diseases of the intestinal and respiratory tracts. *J. Intern. Med.* 2019;285(5):479–490.
6. Johansson MEV, Hansson GC. Immunological aspects of intestinal mucus and mucins. *Nat. Rev. Immunol.* 2016;16(10):639.
7. Hansson GC. Mucins and the Microbiome. <https://doi-org.ucsf.idm.oclc.org/10.1146/annurev-biochem-011520-105053> 2020;89:769–793.
8. Schneider H, et al. Study of mucin turnover in the small intestine by in vivo labeling doi:10.1038/s41598-018-24148-x
9. De Lisle RC, Borowitz D. The Cystic Fibrosis Intestine. *Cold Spring Harb. Perspect. Med.* 2013;3(9):a009753.
10. Hodges CA, et al. Generation of a conditional null allele for CFTR in mice. *genesis* 2008;46(10):546–552.

11. Gustafsson JK, et al. Bicarbonate and functional CFTR channel are required for proper mucin secretion and link cystic fibrosis with its mucus phenotype. *J. Exp. Med.* 2012;209(7):1263–1272.
12. Schütte A, et al. Microbial-induced meprin β cleavage in MUC2 mucin and a functional CFTR channel are required to release anchored small intestinal mucus. *Proc. Natl. Acad. Sci. U. S. A.* 2014;111(34):12396–12401.
13. Kattah MG, et al. A20 and ABIN-1 synergistically preserve intestinal epithelial cell survival. *J. Exp. Med* 2018;215(7):1839–1852.
14. Rusu I, et al. Microbial signals, MyD88, and lymphotoxin drive TNF-independent intestinal epithelial tissue damage. *J. Clin. Invest.* 2022;132(5).
doi:10.1172/JCI154993
15. Leppkes M, et al. Pleiotropic functions of TNF- in the regulation of the intestinal epithelial response to inflammation. *Int. Immunol.* 2014;26(9):509–515.
16. Iwashita J, et al. mRNA of MUC2 is stimulated by IL-4, IL-13 or TNF- α through a mitogen-activated protein kinase pathway in human colon cancer cells. *Immunol. Cell Biol.* 2003;81(4):275–282.
17. Van Hauwermeiren F, et al. TNFR1-induced lethal inflammation is mediated by goblet and Paneth cell dysfunction. *Mucosal Immunol.* 2015 84 2014;8(4):828–840.
18. Sharba S, et al. Interleukin 4 induces rapid mucin transport, increases mucus thickness and quality and decreases colitis and *Citrobacter rodentium* in contact with epithelial cells. *Virulence* 2019;10(1):97–117.

19. Brown KS, et al. Tumor necrosis factor induces developmental stage-dependent structural changes in the immature small intestine.. *Mediators Inflamm.* 2014;2014:852378.
20. McElroy SJ, et al. Tumor necrosis factor receptor 1-dependent depletion of mucus in immature small intestine: A potential role in neonatal necrotizing enterocolitis. *Am. J. Physiol. - Gastrointest. Liver Physiol.* 2011;301(4):G656.
21. Sato T, et al. Single Lgr5 stem cells build crypt–villus structures in vitro without a mesenchymal niche. *Nature* 2009;459. doi:10.1038/nature07935
22. Wajant H, Siegmund D. TNFR1 and TNFR2 in the Control of the Life and Death Balance of Macrophages. *Front. Cell Dev. Biol.* 2019;7:91.
23. Leppkes M, et al. Pleiotropic functions of TNF- in the regulation of the intestinal epithelial response to inflammation. *Int. Immunol.* 2014;26(9):509–515.
24. Almeqdadi M, et al. Gut organoids: Mini-tissues in culture to study intestinal physiology and disease. *Am. J. Physiol. - Cell Physiol.* 2019;317(3):C405–C419.
25. Ruder B, Atreya R, Becker C. Tumour Necrosis Factor Alpha in Intestinal Homeostasis and Gut Related Diseases. *Int. J. Mol. Sci.* 2019;20(8):1887.
26. Keshav S, et al. Tumor necrosis factor mRNA localized to Paneth cells of normal murine intestinal epithelium by in situ hybridization. *J. Exp. Med.* 1990;171(1):327.
27. Tan X, Hsueh W, Gonzalez-Crussi F. *Cellular Localization of Tumor Necrosis Factor (TNF)-a Transcripts in Normal Bowel and in Necrotizing Enterocolitis TNF Gene Expression by Paneth Cells, Intestinal Eosinophils, and Macrophages*
28. Yu S, et al. Paneth Cell Multipotency Induced by Notch Activation following Injury. *Cell Stem Cell* 2018;23(1):46-59.e5.

29. Roda G, et al. Crohn's disease. *Nat. Rev. Dis. Prim.* 2020 61 2020;6(1):1–19.
30. Strugala V, Dettmar PW, Pearson JP. Thickness and continuity of the adherent colonic mucus barrier in active and quiescent ulcerative colitis and Crohn's disease. *Int. J. Clin. Pract.* 2008;62(5):762–769.
31. Pasparakis M, et al. Immune and inflammatory responses in TNF α -deficient mice: A critical requirement for TNF α in the formation of primary B cell follicles, follicular dendritic cell networks and germinal centers, and in the maturation of the humoral immune response. *J. Exp. Med.* 1996;184(4):1397–1411.
32. Norkina O, Burnett TG, De Lisle RC. Bacterial overgrowth in the cystic fibrosis transmembrane conductance regulator null mouse small intestine. *Infect. Immun.* 2004;72(10):6040–6049.
33. Kuang Z, et al. The intestinal microbiota programs diurnal rhythms in host metabolism through histone deacetylase 3. *Science (80-.)*. 2019;365(6460):1428–1434.
34. Reikvam DH, et al. Depletion of Murine Intestinal Microbiota: Effects on Gut Mucosa and Epithelial Gene Expression. *PLoS One* 2011;6(3).
doi:10.1371/JOURNAL.PONE.0017996
35. Fujiyama T, et al. Inhibitory and excitatory subtypes of cochlear nucleus neurons are defined by distinct bHLH transcription factors, Ptf1a and Atoh1. *Development* 2009;136(12):2049–2058.
36. Tian H, et al. Opposing activities of notch and wnt signaling regulate intestinal stem cells and gut homeostasis. *Cell Rep.* 2015;11(1):33–42.

37. Parker A, et al. Cell proliferation within small intestinal crypts is the principal driving force for cell migration on villi. *FASEB J.* 2017;31(2):636–649.
38. Cheng H, Leblond CP. Origin, differentiation and renewal of the four main epithelial cell types in the mouse small intestine V. Unitarian theory of the origin of the four epithelial cell types. *Am. J. Anat.* 1974;141(4):537–561.
39. Krndija D, et al. Active cell migration is critical for steady-state epithelial turnover in the gut. *Science (80-.).* 2019;365(6454):705–710.
40. El Marjou F, et al. Tissue-specific and inducible Cre-mediated recombination in the gut epithelium. *genesis* 2004;39(3):186–193.
41. Grivennikov SI, et al. Distinct and nonredundant in vivo functions of TNF produced by T cells and macrophages/neutrophils: Protective and deleterious effects. *Immunity* 2005;22(1):93–104.
42. Tallapragada NP, et al. Inflation-collapse dynamics drive patterning and morphogenesis in intestinal organoids. *Cell Stem Cell* 2021;28(9):1516-1532.e14.
43. Vonk AM, et al. Protocol for Application, Standardization and Validation of the Forskolin-Induced Swelling Assay in Cystic Fibrosis Human Colon Organoids. *STAR Protoc.* 2020;1(1):100019.
44. Berkers G, et al. Rectal Organoids Enable Personalized Treatment of Cystic Fibrosis. *Cell Rep.* 2019;26(7):1701-1708.e3.
45. Bitam S, et al. An unexpected effect of TNF- α on F508del-CFTR maturation and function. *F1000Research* 2015;4:218.
46. Sanman LE, et al. Generation and Quantitative Imaging of Enteroid Monolayers. *Methods Mol. Biol.* 2020;2171:99–113.

47. Earle KA, et al. Quantitative Imaging of Gut Microbiota Spatial Organization. *Cell Host Microbe* 2015;18(4):478–488.
48. Mehandru S, Colombel JF. The intestinal barrier, an arbitrator turned provocateur in IBD. *Nat. Rev. Gastroenterol. Hepatol.* 2020 182 2020;18(2):83–84.
49. Donaldson GP, Melanie Lee S, Mazmanian SK. Gut biogeography of the bacterial microbiota. *Nat. Publ. Gr.* [published online ahead of print: 2015]; doi:10.1038/nrmicro3552
50. Mitra A, et al. Cell geometry dictates TNF α -induced genome response.. *Proc. Natl. Acad. Sci. U. S. A.* 2017;114(20):E3882–E3891.
51. Tay S, et al. Single-cell NF- κ B dynamics reveal digital activation and analog information processing in cells. *Nature* 2010;466(7303):267.
52. Lee REC, et al. NF- κ B signalling and cell fate decisions in response to a short pulse of tumour necrosis factor. *Sci. Reports* 2016 61 2016;6(1):1–12.
53. Morton PE, et al. TNFR1 membrane reorganization promotes distinct modes of TNF α signaling. *Sci. Signal.* 2019;12(592):2418.
54. Van Hauwermeiren F, et al. TNFR1-induced lethal inflammation is mediated by goblet and Paneth cell dysfunction. *Mucosal Immunol.* 2015;8(4):828–840.
55. Van Hauwermeiren F, et al. Safe TNF-based antitumor therapy following p55TNFR reduction in intestinal epithelium. *J. Clin. Invest.* 2013;123(6):2590–2603.
56. Jiang Y, et al. TNF- α enhances Th9 cell differentiation and antitumor immunity via TNFR2-dependent pathways. *J. Immunother. Cancer* 2019;7(1):1–12.

57. Acharyya S, et al. TNF Inhibits Notch-1 in Skeletal Muscle Cells by Ezh2 and DNA Methylation Mediated Repression: Implications in Duchenne Muscular Dystrophy. *PLoS One* 2010;5(8):e12479.
58. Azuma Y, et al. Tumor Necrosis Factor- α Induces Differentiation of and Bone Resorption by Osteoclasts *. *J. Biol. Chem.* 2000;275(7):4858–4864.
59. Brischetto C, et al. NF- κ B determines Paneth versus goblet cell fate decision in the small intestine. *Dev.* 2021;148(21). doi:10.1242/DEV.199683/273388
60. Dharmani P, Leung P, Chadee K. Tumor Necrosis Factor- α and Muc2 Mucin Play Major Roles in Disease Onset and Progression in Dextran Sodium Sulphate-Induced Colitis. *PLoS One* 2011;6(9):e25058.
61. Van Der Post S, et al. Structural weakening of the colonic mucus barrier is an early event in ulcerative colitis pathogenesis. *Gut* 2019;68(12):2142–2151.
62. Ninnemann J, et al. TNF hampers intestinal tissue repair in colitis by restricting IL-22 bioavailability. *Mucosal Immunol.* 2022 2022;1–19.
63. Smillie CS, et al. Intra- and Inter-cellular Rewiring of the Human Colon during Ulcerative Colitis. *Cell* 2019;178(3):714-730.e22.
64. Yang Q, et al. Cell fate coordinates mechano-osmotic forces in intestinal crypt formation. *Nat. Cell Biol.* 2021;23(7):733–744.
65. Lloyd-Still JD. Crohn's Disease and Cystic Fibrosis. *Dig. Dis. Sci.* 1994;39(4):880–885.

Publishing Agreement

It is the policy of the University to encourage open access and broad distribution of all theses, dissertations, and manuscripts. The Graduate Division will facilitate the distribution of UCSF theses, dissertations, and manuscripts to the UCSF Library for open access and distribution. UCSF will make such theses, dissertations, and manuscripts accessible to the public and will take reasonable steps to preserve these works in perpetuity.

I hereby grant the non-exclusive, perpetual right to The Regents of the University of California to reproduce, publicly display, distribute, preserve, and publish copies of my thesis, dissertation, or manuscript in any form or media, now existing or later derived, including access online for teaching, research, and public service purposes.

DocuSigned by:

Efren Reyes

19E5D85C6F564D3...

Author Signature

8/24/2022

Date